



Kinetic and equilibrium studies of decolorization of effluent of handmade paper industry by low-cost fly ash

Saakshy Agarwal^{b,*}, Shashi Yadav^a, Ashwini Sharma^b, Kailash Singh^c, A.B. Gupta^d

^aDepartment of Chemical Engineering, Banasthali University, Banasthali, Rajasthan, India, email: shashiyadav222@gmail.com

^bKumarappa National Handmade Paper Institute, Ramsinghpura, Sikarpura Road, Sanganer, Jaipur 302019, Rajasthan, India, Tel./Fax: +141 2730369; emails: saakshyagarwal@gmail.com (S. Agarwal), sharmaashwini59@hotmail.com (A. Sharma)

^cDepartment of Chemical Engineering, Malaviya National Institute of Technology, Jaipur 302017, Rajasthan, India, Tel. +141 2713392; email: ksingh.mnit@gmail.com

^dDepartment of Civil Engineering, Malaviya National Institute of Technology, Jaipur 302017, Rajasthan, India, Tel. +141 2713259; email: akhilendra_gupta@yahoo.com

Received 6 November 2015; Accepted 15 February 2016

ABSTRACT

Handmade paper is famous for its bright color made by single dye or admixture of dyes. Handmade paper industry emits colored effluent which requires cost-effective treatment technologies. In the scope of the present paper, studies have been conducted with a simulated dye solution having a mixture of dyes being used in the handmade paper industry. The original fly ash and adsorbed fly ash were characterized for SEM-EDX, XRD, and Fourier transform infrared (FTIR) studies. The FTIR studies of direct dyes used in mixture (direct orange, direct navy blue, and direct violet dye) were conducted. The batch studies were conducted with low-cost fly ash and various affecting parameters, i.e. pH, initial concentration, temperature of the dye solution, dosage, and particle size of fly ash. The maximum adsorption capacity of fly ash was found to be 120.48 mg/g with fly ash dosage of 40 g/L having particle size of 45–75 μm with dye solution at pH 2 and 40°C temperature. The better coefficient value of R^2 showed better fitting of the Langmuir isotherm with the experimental data. The kinetic sorption data are well represented by the pseudo-second-order kinetics for the entire sorption period. The change in enthalpy, entropy, and free energy were evaluated which indicated that the sorption process is endothermic, spontaneous, and feasible. The characteristics of the effluent of handmade paper industry after fly ash treatment in batch study confirm the acceptability of the use of fly ash for treatment of effluent of handmade paper industry.

Keywords: Handmade paper industry; Fly ash; Mixture of direct dyes; Isotherm; Batch study; Kinetics

*Corresponding author.

1. Introduction

Water is the basic necessity to sustain life, but the rapid growth in industrialization has led to pollution of water at a speeding rate, thus making it a major environmental issue worldwide. The effluent generated by the textile industries, dye manufacturing industries, paper and pulp industries contains large quantities of dangerous pollutants like dyes, pigments, and heavy metals [1] which when discharged into the water bodies cause serious water pollution. Approximately, 10,000 different dyes and pigments are used for industries, most of which are difficult to biodegrade since they have complex aromatic molecular structure and synthetic origin [2]. The presence of dyes in wastewater reduces sunlight penetration thus having an adverse effect on photosynthesis and aquatic life. Moreover, reactive dyes that are chemically stable and having little biodegradability are likely to pass untreated through conventional treatment methods, thus rendering these methods unsuitable for the treatment of colored effluent. But, it is imperative to remove dyes because of their toxic effects: mutagenesis, chromosomal fractures, carcinogenesis, and respiratory toxicity [3]. Several methods are being used for their removal like adsorption, precipitation, coagulation, flocculation, reverse osmosis, biological process, ionizing, gamma radiations, and photocatalysis. However, the disadvantage of these methods is that they are expensive. Among all the above treatment methods, adsorption is found to be the most appropriate technique because of its easy operation and well-known technology, inexpensive equipment, and less sludge [4]. Moreover, the adsorbents can be chosen from a wide variety including fly ash, sepiolite, mud, clay, activated carbon, etc. Granular activated carbon is the most popular adsorbent and has been used with great success [5]. However, desorption and regeneration of dyes is difficult under common conditions because of which the overall process becomes expensive thus restricting its large-scale application. This has led many researchers to do research in the field of low-cost adsorbents.

Fly ash is a byproduct of the combustion of pulverized coal generated in large quantities in electric power generation plants. It contains many hazardous substances and feces disposal problems. It is widely used in concrete, brick manufacture, road sub-base, and mine backfill. Although its use in construction and other civil engineering applications is expected to increase, it is unlikely that it will use all the generated fly ash [6]. Therefore, continuous research is required to further exploit the potential of fly ash. Previous studies have been conducted on fly ash as

low-cost adsorbent by other researchers [7–9]. The adsorption capacity of fly ash depends on the surface area of fly ash. Fly ashes collected in electrostatic precipitators have shown surface areas of 0.40–0.70 m²/g, cyclone-collected (mechanically collected) ashes varies between 0.15 and 0.20 m²/g [10]; 10–60 m²/g [11]; 0.75–0.8 m²/g [12]. Sludge containing dyes is not easy for disposal as it contains “hazardous substances”. Studies are available on handling such sludges, the solidification–stabilization being the most prominent among such technologies [13,14]. The present study intends to incorporate the sludge in bricks and study the engineering properties of such bricks as well as their environmental acceptability as per Toxicity Characteristic Leaching Procedures recommended by the USEPA. The present study aims to increase the scope of application of raw coal fly ash in the removal of dyes from colored effluent generated by the pulp and paper industries. The effect of adsorbent dosage, particle size of adsorbent, initial pH, temperature, and initial concentration was investigated to determine the optimum conditions for dye removal. Experimental equilibrium data were fitted to Langmuir and Freundlich isotherms to determine the best fit isotherm equation. Adsorption kinetics has been studied using pseudo-first-order and pseudo-second-order kinetic models. Thermodynamic studies have been done to determine the change in Gibbs free energy, enthalpy, and entropy.

2. Materials and methods

2.1. Fly ash preparation

Fly ash was procured from a thermal power plant at Yamuna Nagar. Fly ash was washed with distilled water and dried in oven at 103°C for 3 h. Fly ash of different size was prepared with the help of ash sieve shaker by passing ash through sieves of ASTM no. 50, 80, 100, 200, and 300 and then finally collected in polyethylene bags for experimental studies.

2.2. Simulation of effluent of handmade paper industry

A stock of a mixture of commercial dyes, i.e. Direct Orange 26, Direct Navy Blue 6, and Direct Violet 66 was simulated in the laboratory in a specific ratio to give desired shade used in the handmade paper industry and treated as a stock solution of 1,000 mg/L. The stock solution was preserved and used for further studies by dilution of stock solution.

2.3. Characterization of fly ash

2.3.1. SEM characterization

The surface morphology of raw and adsorbed fly ash samples was characterized by Scanning Electron Microscopy (Nova Nano FE-SEM 450 FET) with accelerating voltage of 5 kV and magnification of 500× to 5,000× and field emission gun SEM. The FESEM is coupled to an Energy-Dispersive X-ray (EDX) detector for measuring the elemental composition. The particles were slightly carbon coated before analysis to make its surface more conductive. X-ray analysis was done in spot mode at 25 kV.

2.3.2. FTIR studies of fly ash

Fourier transform infrared (FTIR) was carried out at room temperature using Perkin Elmer version 10.4 Spectrophotometer in the spectral range of 4,000–400 cm^{-1} having resolution of 4 cm^{-1} with KBr disc method.

2.3.3. Mineralogical composition of fly ash by XRD

The XRD studies of original fly ash and adsorbed fly ash were conducted with the help of X-ray Diffractometer (Panalytical X Pert Pro) with Cu K α radiation with wavelength λ of 1.540 Å, step scans with 0.03° step and 1 s.

2.4. Characterization of effluent of handmade paper industry

The effluent of handmade paper industry using a mixture of dyes was scanned from 400 to 1,000 nm with the help of double-beam UV–vis spectrophotometer and λ_{max} was found to be 554 nm. The standard curve at maximum wavelength, i.e. 554 nm has been prepared at different initial concentration of the simulated colored effluent and Beer–Lambert law was found to follow up to 200 mg/l dye solution. The concentration of dye was determined in the effluent of handmade paper industry. The effluent of handmade paper industry was characterized for chemical oxygen demand, biochemical oxygen demand, and color as per standard testing method of water and wastewater.

2.5. Experimental setup

The fly ash of various particle sizes ASTM 50–80 (180–300 μm), ASTM 80–100 (150–180 μm), ASTM 100–200 (75–150 μm), and ASTM 200–300 (45–75 μm) was taken for decolorization studies of dye solution of var-

ious concentrations, i.e. 44.65, 89.3, 119.06, 127.57, 178.6 mg/l and fly ash dosage varying from 8, 14, 32, 40 g/L and at 20, 25, 30, 35, and 40°C temperature. The specific amount of fly ash dosage was fed to a specific amount of dye solution in the Erlenmeyer conical flask of 250 ml capacity and was mixed with the help of thermostatically controlled cabinet at 150 RPM. The initial pH of the dye solution was maintained at 2, 4, 6, 8, and 10 with the help of 1 N NaOH and 1 N HCl to study the effect of pH on the decolorization efficiency of fly ash. The spent liquor was collected after every 5 min until no further change in color was observed. The collected samples were then centrifuged at 1,350 RPM for 10 min to get a clear solution for spectrophotometric analysis. The supernatant was collected for determination of the absorbance at a maximum wavelength with the help of double-beam UV–vis Spectrophotometer, ECA Hyderabad.

The percentage decolorization was calculated by the following equation [15]:

$$\text{Decolorization (\%)} = 100 \frac{(C_o - C_e)}{C_o} \quad (1)$$

where C_o represents the initial concentration of the dye and C_e represents the equilibrium concentration.

The amount adsorbed was calculated by the given equation [16]:

$$\text{Amount adsorbed, } q_e \text{ (mg/g)} = \frac{(C_o - C_e)V}{M} \quad (2)$$

3. Results and discussions

3.1. Characterization of fly ash

The fly ash has been characterized by SEM, FTIR, and XRD studies.

3.1.1. Scanning electron microscopic studies

The fly ash particles analyzed by SEM equipped with EDX showed the shape and structure of fly ash particles along with the chemical composition before and after adsorption (Fig. 1). The morphology of raw fly ash in Fig. 1 showed spherical shape and small size of fly ash particles. The elemental composition of fly ash before adsorption and after adsorption is shown in Fig. 2, which indicates the presence of Zr, Fe, Al, Si, O, and additional K and C element after adsorption. The adsorbed fly ash showing different embedded elements is shown in Fig. 3 at 100,000× magnification. The elemental analysis of fly ash is shown as Table 1.

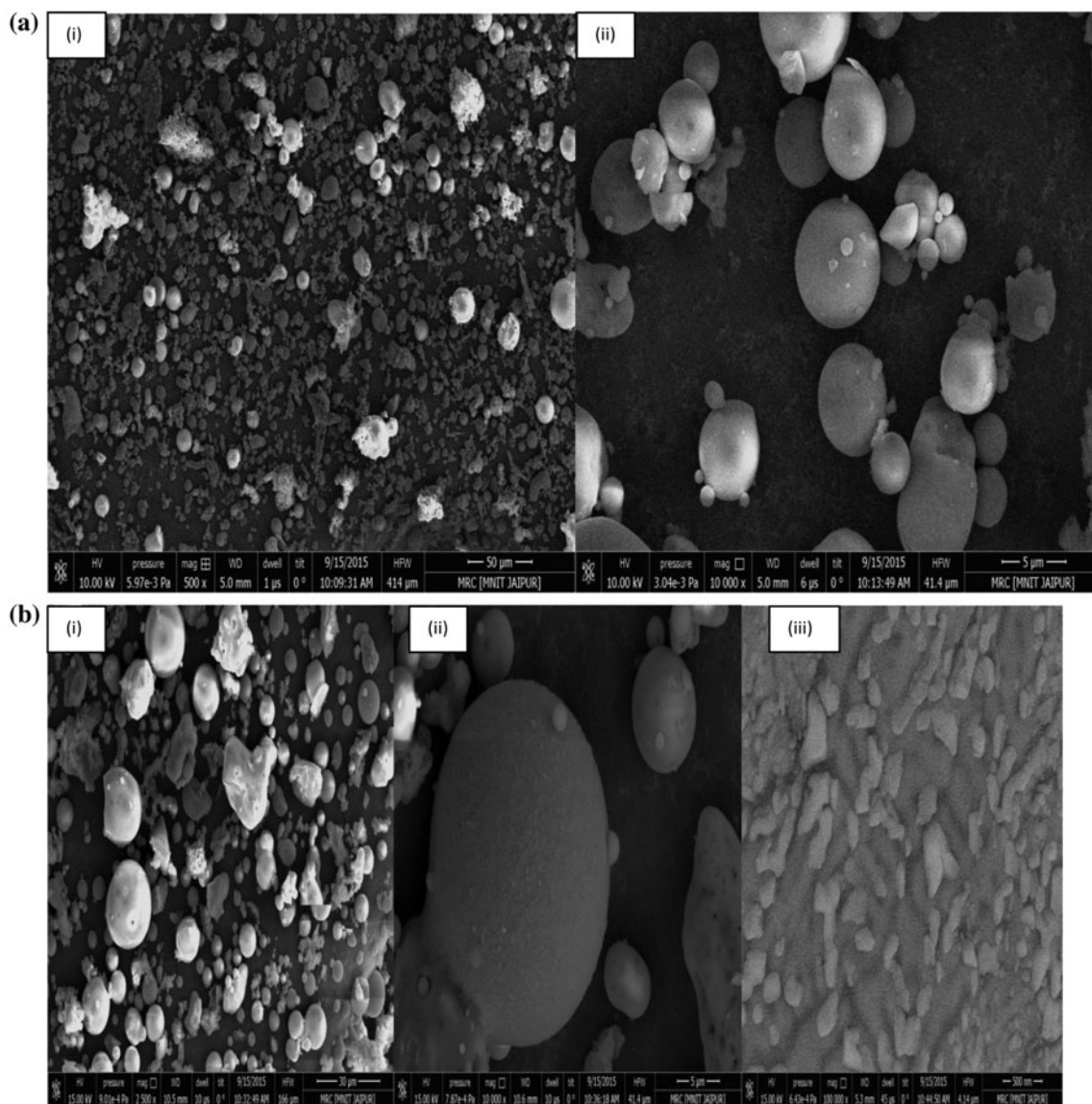


Fig. 1. SEM image of (a) raw fly ash at (i) 500 \times , (ii) 10,000 \times magnification and (b) adsorbed fly ash at (i) 2,500 \times , (ii) 10,000 \times , and (iii) 100,000 \times magnification.

3.1.2. XRD studies

The mineralogical composition of original fly ash and adsorbed fly ash is given in Fig. 4.

The diffraction peaks showed that fly ash consisted mainly of crystalline phases such as quartz (SiO_2), alumina (Al_2O_3), and hematite (Fe_2O_3), while adsorbed fly ash consisted of crystalline quartz (SiO_2), and new crystalline phase of aluminum silicate.

3.1.3. Fourier transform infra-red studies

The FTIR study from Fig. 5 showed primary aliphatic amines of band from 3,250 to 3,450 cm^{-1} in

adsorbed fly ash due to adsorption of aliphatic amines of mixture of dyes on fly ash. The FTIR spectra of adsorbed fly ash indicated strong broadband in the region of 1,600–1,800 cm^{-1} due to C=O group stretching bands from aldehydes and ketones in dye-adsorbed fly ash. The intense vibration at 600–400 cm^{-1} attributes to silicate minerals in raw and adsorbed fly ash. The C–N stretching absorption of aliphatic amines occurs in the region 1,090–1,020 cm^{-1} to higher frequency in adsorbed fly ash. The C–H stretching can be found in adsorbed fly ash between 2,541 and 2,973 cm^{-1} due to aliphatic hydrocarbon. The C–C stretching of 1,579–1,652 cm^{-1} was found in both raw and adsorbed fly ash. The stretching of

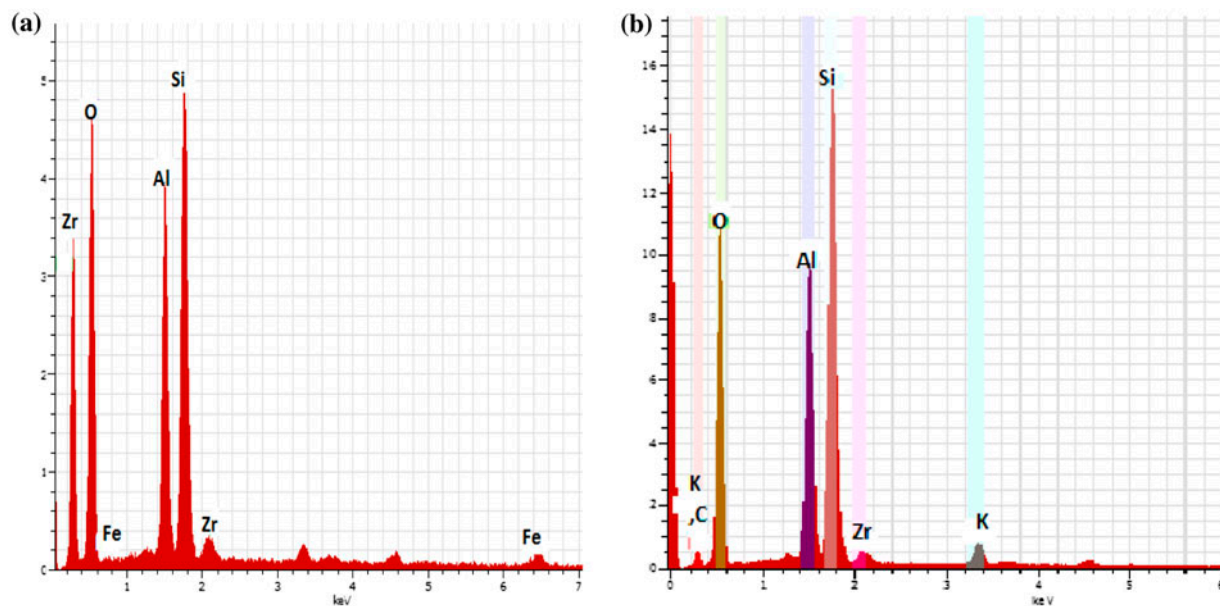


Fig. 2. (a) SEM-EDX of original fly ash and (b) EDX of adsorbed fly ash.

Si–O quartz is attributed to $1,079.77\text{ cm}^{-1}$ in original fly ash and $1,089, 796.08\text{ cm}^{-1}$ in adsorbed fly ash. The stretching of Si–O–Al is attributed to 558.38 cm^{-1} in original fly ash and 561.70 cm^{-1} to adsorbed fly ash.

3.2. Characterization of dye

The dye solution of direct orange 26, direct navy blue 2, and direct violet 66 was scanned from 200 to 1,000 nm with the help of double-beam UV–vis spectrophotometer. The characteristic of dyes is summarized in Table 2. The maximum absorbance was obtained for direct orange 26, direct navy blue 6, and direct violet 66 at wavelength of 491; 569 and 525; 625 nm, respectively, while the maximum absorbance for mixture of dyes was obtained at single wavelength of 509 nm. The standard calibration chart of mixture of dyes of various concentrations was prepared for determination of concentration of black dye solution by analyzing the absorbance at respective maxima. It was also found that Beer's law was followed for dye concentrations up to 200 mg/L.

3.2.1. FTIR studies of direct dyes

The FTIR peaks can be seen in Fig. 6. The $1,508\text{--}1,396\text{ cm}^{-1}$ can be assigned to the antisymmetric CO_3 stretching band in direct orange, while at $1,100\text{ cm}^{-1}$

in direct violet can be assigned to the symmetric carbonate mode, and bands at $894\text{--}797\text{ cm}^{-1}$ are assigned to the vibrational modes of goethite in direct orange and direct violet dye. The presence of vibrational bands in the $3,000\text{ cm}^{-1}$ region as well as bands in the $1,300\text{--}1,000\text{ cm}^{-1}$ region is an indication of organic components or functionality present in direct orange, direct navy blue, and direct violet dye. Several bands in the region between $1,600$ and $1,000\text{ cm}^{-1}$ are characteristic of the organic aromatic group. Hydrocarbons show absorption peaks between $2,800$ and $3,300\text{ cm}^{-1}$ due to C–H stretching vibrations in direct orange, direct navy blue, and direct violet dye. Primary amines contain –NH_2 group (N–H bonds) stretch from $3,100$ to $3,500\text{ cm}^{-1}$. Benzene rings often give characteristic absorptions at about $680\text{--}900\text{ cm}^{-1}$ in direct orange and direct violet dye. The *o*-substituted pattern of benzene ring can be seen in direct violet dye as a single peak between 735 and 770 cm^{-1} . C–H bonds absorb in the range of $2,853\text{--}2,962\text{ cm}^{-1}$ in direct navy blue and direct violet dye. The OH absorptions are generally quite intense and smoothly curved in the range of $2,500\text{--}3,300\text{ cm}^{-1}$. Ethers have a C–O stretch that appears in the fingerprint region at $1,050\text{--}1,260\text{ cm}^{-1}$. This is generally a strong absorption, but can be difficult to detect if the fingerprint region is complex. Alcohols, esters, and other compounds containing C–O single bonds also show a C–O stretch in this region.

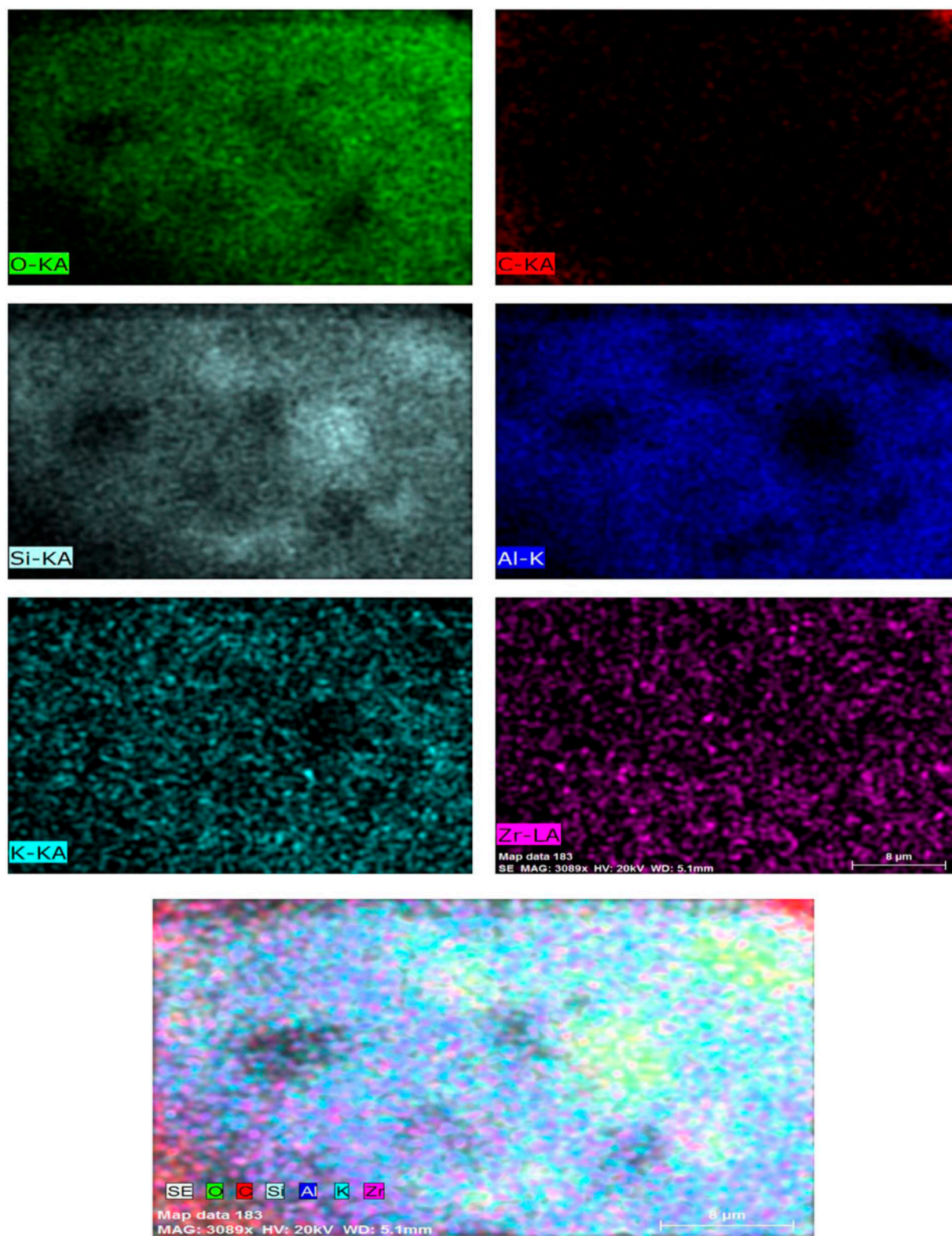


Fig. 3. Different elements (O, C, Si, Al, K, and Zr) in adsorbed fly ash at 100,000× magnification.

Table 1
Elemental analysis of fly ash

Element	Original fly ash				Adsorbed fly ash			
	Unn. C (wt.%)	Norm. C (wt.%)	Atom. C (at.%)	Sigma (wt.%)	Unn. C (wt.%)	Norm. C (wt.%)	Atom. C (at.%)	Sigma (wt.%)
O	32.11	56.71	71.29	4.67	44.79	53.85	63.04	5.22
Si	11.61	20.51	14.69	0.54	7.34	20.84	13.90	0.77
Al	9.39	16.58	12.36	0.50	11.44	13.76	9.55	0.57
Zr	2.34	4.13	0.91	0.16	1.79	2.15	0.44	0.10
Fe	1.17	2.07	0.74	0.09				
K					1.23	1.48	0.71	0.07
Total	79.96	100	100		83.18	100	100	

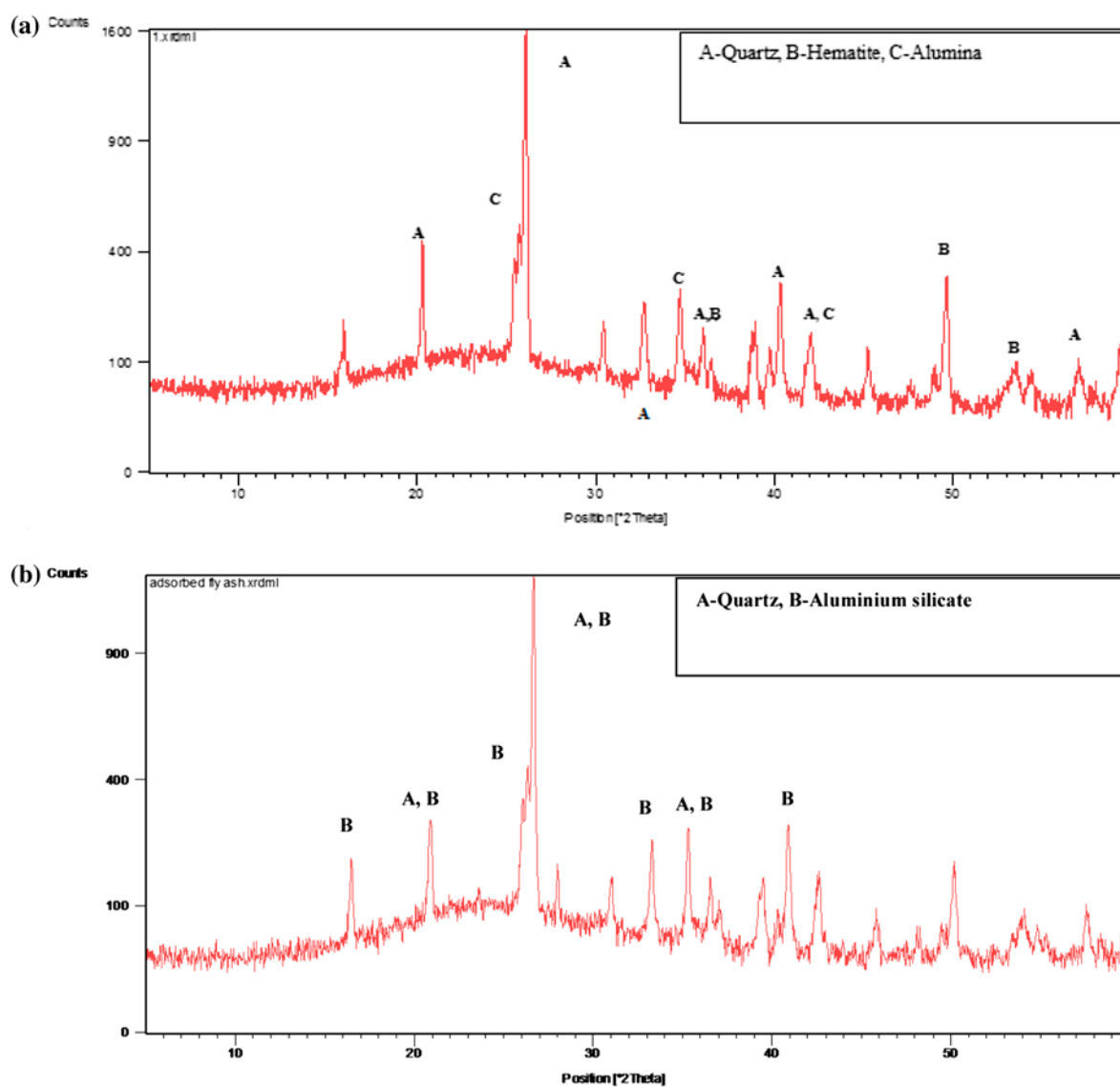


Fig. 4. X-ray diffraction pattern of (a) raw fly ash and (b) fly ash adsorbed with mixture of dyes.

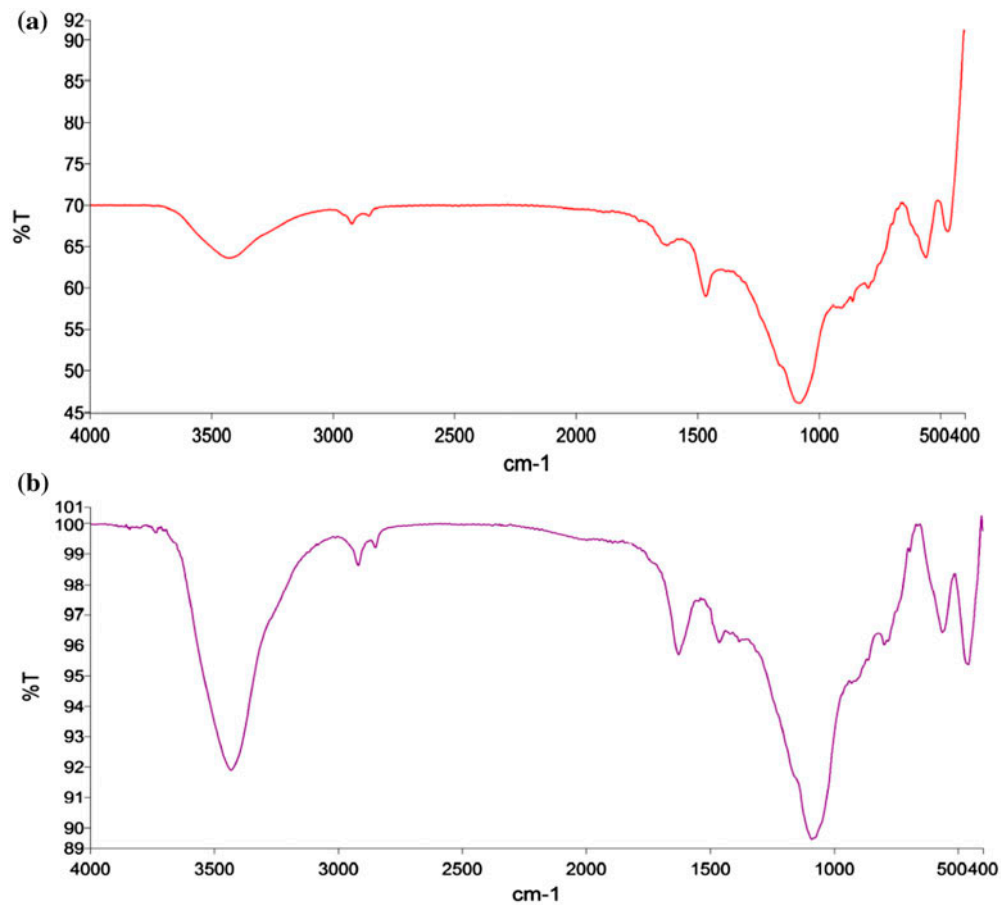


Fig. 5. FTIR spectra of (a) raw fly ash and (b) adsorbed fly ash with mixture of dyes.

Table 2
Characteristics of direct dyes

Chemical name	Direct orange	Direct navy blue	Direct violet
pH	7.78	7.98	7.34
Type	Anionic	Anionic	Anionic
λ_{\max} (nm)	491	569	525
Insoluble matter (%)	6.78	4.56	5.45
Color index	40,220	22,610	29,120
Molecular weight	756.67	932.76	903.81

3.3. Effect of parameters

3.3.1. Effect of fly ash dosage

The effect of fly ash dosage on decolorization of dye solution of initial concentration 178.6 mg/l maintained at 25°C and pH 7.5 is shown in Fig. 7. It

was observed that the decolorization efficiency of fly ash increased with the increase in dosage of fly ash. The decolorization of dye solution obtained by 8, 16, 32, and 40 g/l dosage of fly ash at 45 min was 36.7, 38.5, 46.5, and 50.6%, respectively. The increase in adsorption efficiency of fly ash with increase in

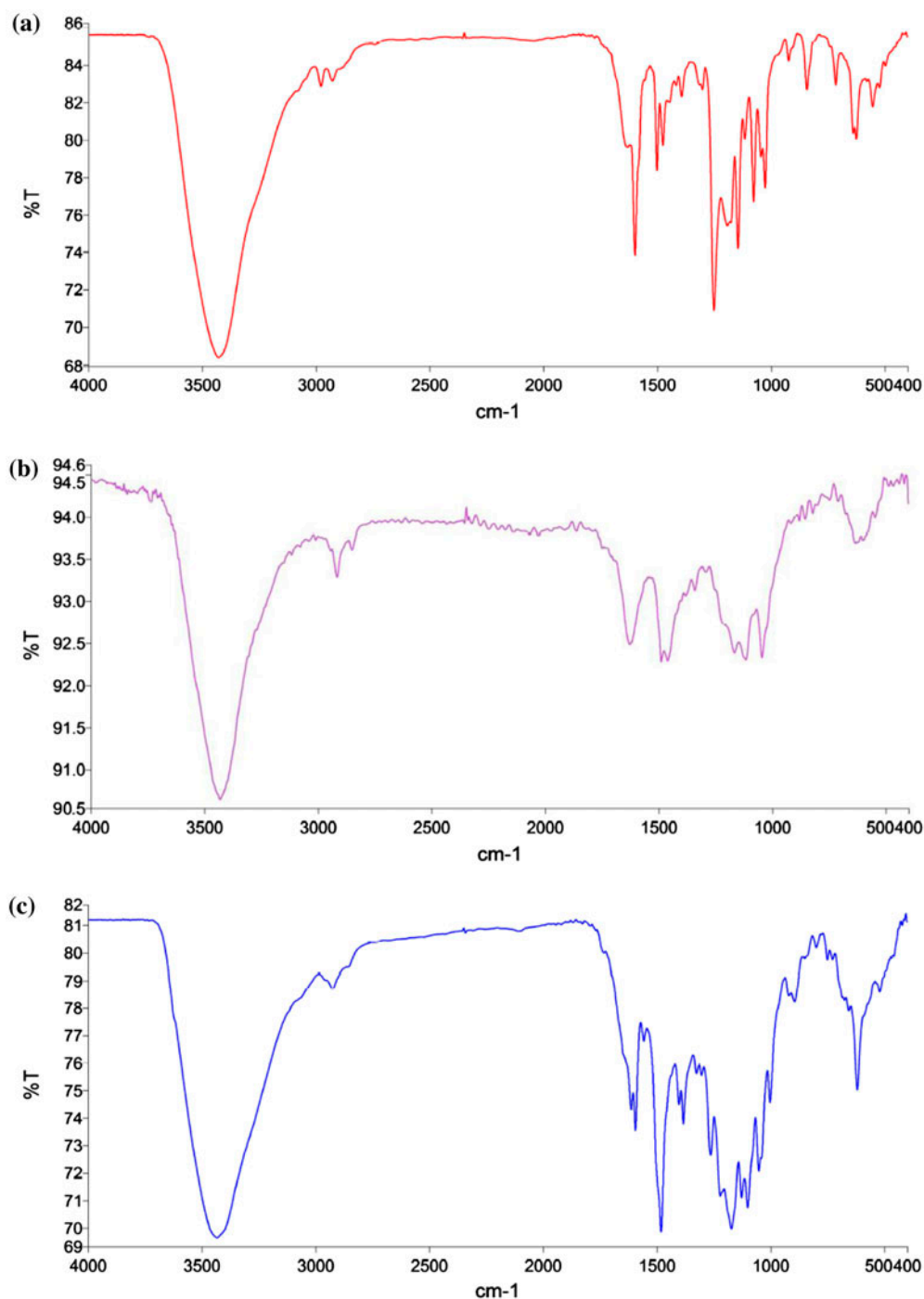


Fig. 6. FTIR spectra of (a) Direct Orange 26, (b) Direct navy blue 6, and (c) Direct Violet 66.

dosage was probably because with the increase in the adsorbent dosage, the number of active sites available for adsorption of dye increased. Similar results have been reported previously by Mall et al. [17].

3.3.2. Effect of particle size of fly ash

The effect of various particle size of fly ash ASTM 50–80 (180–300 μ), ASTM 80–100 (150–180 μ), ASTM 100–200 (75–150 μ), and ASTM 200–300 (45–75 μ) was studied at 25°C with initial dye concentration of

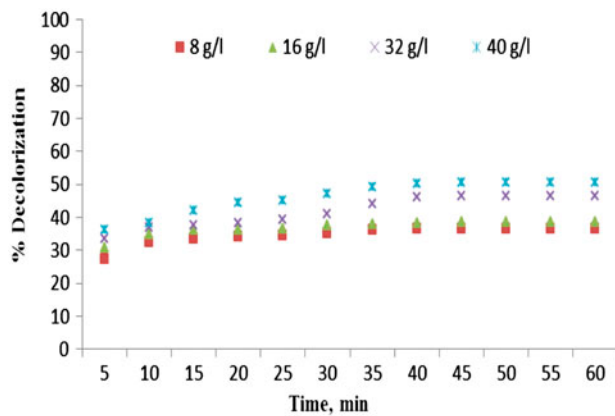


Fig. 7. Effect of adsorbent dosage (initial concentration of dye: 178.6 mg/l, pH 7.5, temperature: 25°C).

178.6 mg/l and fly ash dosage of 40 g/l. The effect of various particle size of fly ash on decolorization of a dye solution is shown in Fig. 8. It was observed from Fig. 8 that the decolorization of dye solution increased with the decrease in the particle size of fly ash because smaller particles have relatively larger surface area and therefore offer more adsorption sites. Similar results have been reported by Kara et al. [18]. The maximum percentage reduction in color, obtained by fly ash of particle size 45–75 μ was 55.7% at 45 min.

3.3.3. Effect of pH

The effect of decolorization efficiency of fly ash (40 g/l and 45–75 μ particle size) with dye solution of 178.6 mg/l initial concentration at various pH 2, 4, 6, 8, 10 at 25°C is shown in Fig. 9. It has been observed

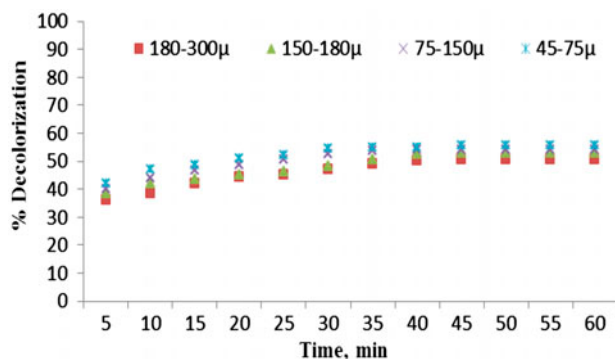


Fig. 8. Effect of particle size of adsorbent (initial concentration of dye: 178.6 mg/l, fly ash dosage: 40 g/l, pH 7.5, temperature: 25°C).

that the decolorization of dye solution was maximum at extreme pH, i.e. at pH 2. It is because by decreasing the pH, fly ash surface becomes protonated or positively charged. Since the dyes used were anionic, at low pH, an attractive force develops between the positively charged adsorbent surface and negatively charged dye particles which results in an increased adsorption [19]. The percentage reduction in colorant at an initial pH of 2, 4, 6, 8, and 10 was 88.5, 66.9, 66.7, 62.8, and 84.3%, respectively, at 45 min.

3.3.4. Effect of temperature

The effect of various temperature of dye solution, i.e. 20, 25, 30, 35, and 40°C and an initial concentration of 178.6 mg/L maintained at pH 2 on the decolorization efficiency of fly ash is shown in Fig. 10. From the figure, it has been found that the percentage color removal increased with the increase in temperature. The percentage reduction in color, obtained by treating effluent at temperature 20, 25, 30, 35, and 40°C was 81.8, 87.5, 89.5, 90.3, and 93.5%, respectively, at 45 min. The increase in adsorption with increase in temperature is attributed to increase in mobility of the dye molecules with increase in temperature. It may be due to the interaction between the dye molecules and the active sites of the adsorbent increases [20]. Moreover, increasing temperature may produce a swelling effect within the internal structure of the fly ash, which will increase the pore size and consequently adsorption also [21].

3.3.5. Effect of initial concentration

The effect of initial concentration of dye solution at various concentrations 44.65, 89.3, 119.06, 127.57, and

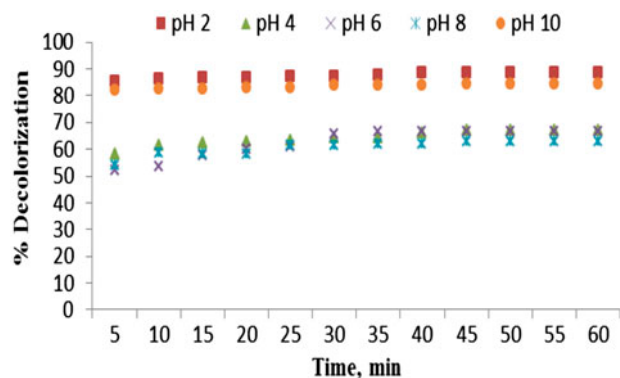


Fig. 9. Effect of pH (initial concentration of dye: 178.6 mg/l, fly ash dosage: 40 g/l, particle size: 45–75 μ , temperature: 25°C).

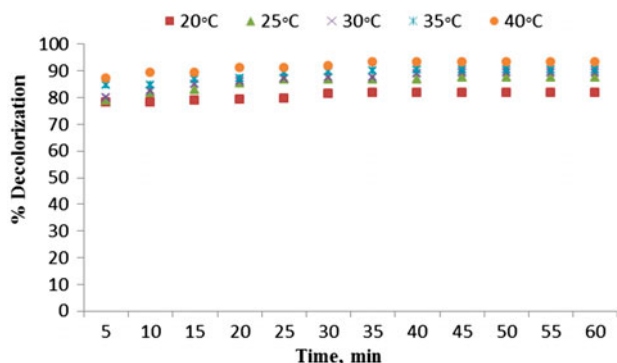


Fig. 10. Effect of temperature (initial concentration of dye: 178.6 mg/l, fly ash dosage: 40 g/l, particle size: 45–75 μ, pH 2).

178.6 mg/l on the decolorization efficiency of fly ash of particle size 45–75 μ and 40 g/l dosage is shown in Fig. 11. It has been observed that the decolorization of dye solution decreased with the increase in initial dye concentration. At low concentrations, the number of adsorbate molecules was less, while at high concentrations, the number of adsorbate molecules was more as compared to the active sites on the adsorbent. Thus, with the increase in the concentration of the dye, the competition for active sites of adsorbent increases, and as a result, complete removal of dye takes longer time at higher concentrations than at lower concentrations of the dye [22]. Thus, at high concentrations, the amount of dye adsorbed is less, and as a result, percentage removal is also low. The percentage reduction in color, obtained by treating effluent having initial concentrations 44.6, 89.3, 119, 127.5, and 178.6 mg/l was 99, 98.5, 96.2, 95.3 and 93.5%, respectively, at 45 min.

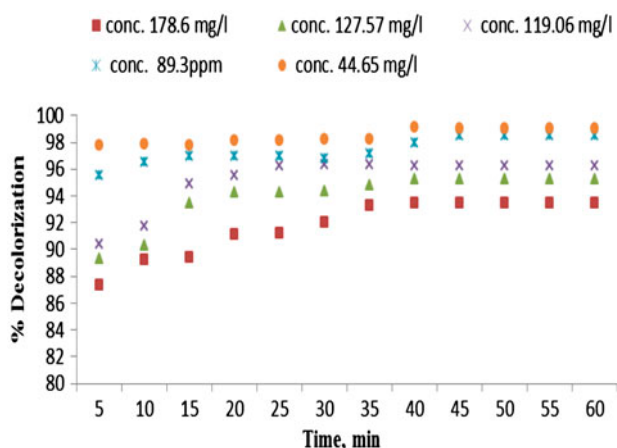


Fig. 11. Effect of initial concentration (fly ash dosage: 40 g/l, particle size: 45–75 μ, pH 2, temperature: 40°C).

3.4. Adsorption equilibrium

Equilibrium data are important for designing an adsorption system. The equilibrium data were analyzed using Langmuir, Freundlich, Temkin, and Dubinin–Radushkevich isotherms.

3.4.1. Langmuir isotherm

Langmuir isotherm assumes monolayer adsorption on specific homogeneous sites. The linearized Langmuir isotherm is represented by Eq. (3) [23]:

$$\frac{1}{Q_e} = \frac{1}{C_e K_L Q_{max}} + \frac{1}{Q_{max}} \quad (3)$$

The value of the dimensionless separation factor R_L is calculated by the following equation:

$$R_L = \frac{1}{1 + K_L C_o} \quad (4)$$

The Langmuir isotherm plot is given in Fig. 12.

3.4.2. Freundlich isotherm

Freundlich isotherm assumes adsorption on heterogeneous surface and multilayer adsorption. The linearized Freundlich isotherm is represented by Eq. (5) [24]:

$$\ln Q_e = \ln K_F + \frac{1}{n} \ln C_e \quad (5)$$

Fig. 13 exhibits Freundlich isotherm plot for the adsorption of dyes on fly ash.

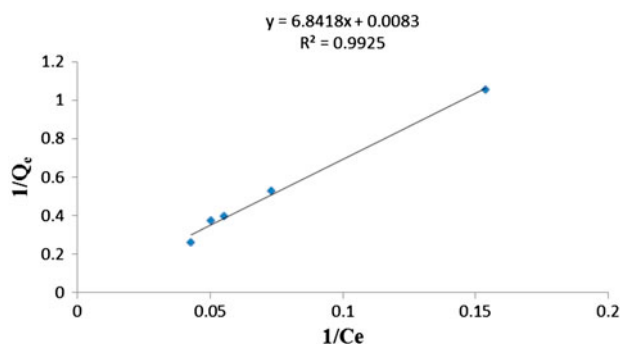


Fig. 12. Langmuir adsorption isotherm (temperature: 40°C; pH 2.0; fly ash dosage: 40 g/l; time: 45 min).

3.4.3. Temkin isotherm

Temkin isotherm takes into the account of adsorbent–adsorbate interactions [25,26] and is given by the following equation:

$$q_e = B_T \ln A_T + B_T \ln C_e \quad (6)$$

A linear fitting of q_e vs. $\ln C_e$ enables the determination of isotherm constants A_T and B_T is given in Table 3. A comparison of R^2 values of the three isotherms indicates that Langmuir isotherm is the best fitted.

3.4.4. Dubinin–Radushkevich isotherm

Dubinin–Radushkevich isotherm expresses the adsorption mechanism with a Gaussian energy distribution onto a heterogeneous surface [27,28] and to estimate the characteristic porosity of the adsorbent and apparent energy of adsorption [29]:

$$\ln q_e = \ln q_s - K_{ad}\varepsilon^2 \quad (7)$$

$$\varepsilon = RT \ln \left(1 + \frac{1}{C_e} \right) \quad (8)$$

The approach was usually applied to distinguish the physical and chemical adsorption of metal ions with its mean free energy, E per molecule of adsorbate (for removing a molecule from its location in the sorption space to the infinity) can be computed by the relationship [30,31]:

$$E = \frac{1}{\sqrt{2B_{DR}}} \quad (9)$$

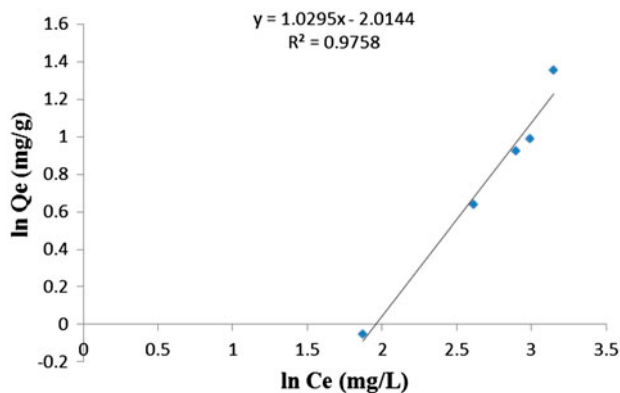


Fig. 13. Freundlich adsorption isotherm (temperature: 40 °C, pH 2.0, fly ash dosage 40 g/l, time: 45 min).

One of the unique features of the Dubinin–Radushkevich (DRK) isotherm model lies on the fact that it is temperature-dependent, which, when adsorption data at different temperatures are plotted as a function of the logarithm of the amount adsorbed, $\ln q_e$ vs. ε^2 the square of potential energy, all suitable data will lie on the same curve, named as the characteristic curve [32]. The Langmuir, Freundlich, Temkin, and Dubinin–Radushkevich isotherm constants are presented in Table 3. It was observed that the equilibrium data fitted better with a Langmuir model for adsorption of mixture of direct dyes on fly ash with better correlation coefficient value of 0.993. The higher correlation coefficient of the Langmuir isotherm predicts the monolayer coverage of dye mixture of fly ash particles. The value of R_L is 0.8219. Since the value of R_L lies between 0 and 1, adsorption using coal fly ash is favorable. The values of K_F and n were calculated from the intercept and slope of the plot of $\ln q_e$ vs. $\ln C_e$ and the values of Q_{max} and K_L were calculated from the intercept and slope of the plot of $1/q_e$ vs. $1/C_e$. From Table 3, it was seen that the maximum sorption capacity Q_{max} (mg/g) of fly ash for the mixture of dyes was 120.482 mg/g. The E value of 0.7 kJ/mol from Dubinin–Radushkevich model indicates adsorption of a mixture of dyes on fly ash as physisorption process [33].

3.5. Adsorption kinetics

The kinetics of adsorption of a mixture of dyes onto fly ash was modeled by the pseudo-first-order Lagergren equation, pseudo-second-order model, intraparticle diffusion, and Bangham kinetics.

3.5.1. Pseudo-first-order kinetics

The Lagergren first-order model is given by the following equation [34]:

$$\log(q_e - q_t) = \log q_e - \frac{K_{ad}t}{2.303} \quad (10)$$

The value of K_{ad} was obtained from the Lagergren plot of $\log(q_e - q_t)$ vs. t for different dye concentrations ranging from 44.65 to 178.6 mg/L.

3.5.2. Pseudo-second-order kinetics

The second-order kinetics model proposed by Ho and McKay is expressed as equation [35]:

$$t/q_t = t/q_e + 1/k_2q_e^2 \quad (11)$$

Table 3

Isotherm constants for the adsorption of dyes onto fly ash at pH 2 and 40°C

Langmuir isotherm	Freundlich isotherm	Temkin isotherm	Dubinin–Radushkevich isotherm
$Q_{\max} = 120.482 \text{ mg/g}$	$K_F ((\text{mg/g})/(\text{mg/L})^{1/n}) = 0.1334$	$A_T (\text{L/mg}) = 20$	$E (\text{kJ/mol}) = 0.707$
$K_L (\text{L/mg}) = 1.213$	$1/n = 0.971$	$B_T = 0.068$	$q_s (\text{mg/g}) = 3.508$
$R^2 = 0.993$	$R^2 = 0.976$	$R^2 = 0.970$	$R^2 = 0.927$

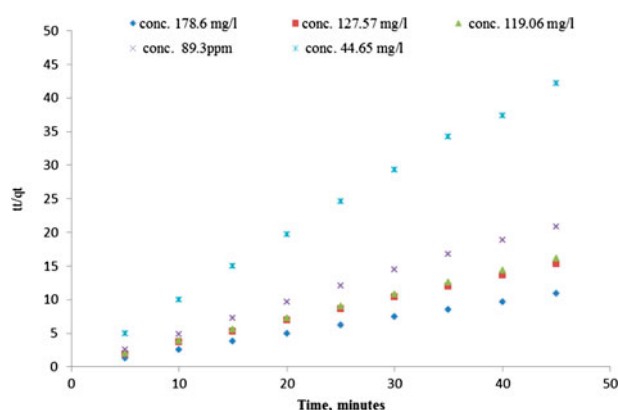


Fig. 14. Pseudo-second-order-plot for adsorption of mixture of dyes with fly ash (temperature: 40°C; pH 2.0; dose 40 g/L; time 45 min).

Values of k_2 and q_e were calculated from intercept and the slope of the linear plots of t/q_t vs. t . The initial adsorption rate, h (mg/g min), at $t \rightarrow 0$, is defined as $h = k_2 q_e^2$.

Fig. 14 shows the pseudo-second-order plot for the mixture of dyes onto fly ash particles. The pseudo-second-order rate constant k_2 , the calculated h value, and the corresponding linear regression correlation coefficient values R^2 are given in Table 4. From Table 4, it was noticed that at all initial dye concentrations and for the entire sorption period, the linear regression correlation coefficient R^2 values were found to be higher. The higher R^2 values confirm that the sorption

data are well represented by the pseudo-second-order kinetics for the entire sorption period and thus supports the assumption behind the model that the sorption is due to chemisorption, which is in good agreement with the sorption equilibrium data well represented by the Langmuir isotherm equation.

3.5.3. Intraparticle diffusion

The intraparticle diffusion model proposed by Weber and Morris is given as:

$$q_t = k_{id} t^{1/2} + C \quad (12)$$

A plot of q_t vs. $t^{1/2}$ gives slope k_{id} and intercept C at different concentrations as given in Table 4. The high correlation coefficient indicates the presence of intraparticle diffusion as the rate-determining step.

3.5.4. Bangham kinetics

The Bangham equation is given in the following form [36]:

$$\log \log \left(\frac{C_o}{C_o - q_t m} \right) = \log \left(\frac{k_0 m}{2.303 V} \right) + \alpha \log(t) \quad (13)$$

The R^2 value less than 0.98 shows that the adsorption of adsorbate into pores of the sorbent is not the only

Table 4

Adsorption rate constants for adsorption at different initial concentrations

C_o (mg/L)	Pseudo-first-order kinetics			Pseudo-second-order kinetics			Intraparticle diffusion		Bangham constants			
	q_e (mg/g)	K_{ad} (1/min)	R^2	k_2 (g/mg min)	h (mg/g min)	R^2	k_{id} (mg/g min ^{0.5})	R^2	α	k_0 (ml/(g/L))	R^2	
44.65	0.078	0.228	0.954	0.395	0.400	0.999	0.013	0.613	0.108	0.045	0.454	
89.3	0.160	0.045	0.621	0.116	3.129	0.999	0.022	0.771	0.103	0.049	0.776	
119.06	0.344	0.310	0.976	0.054	5.669	0.999	0.079	0.836	0.232	0.03	0.917	
127.57	0.436	0.197	0.914	0.410	2.435	0.999	0.078	0.886	0.202	0.031	0.940	
178.6	0.763	0.221	0.763	0.312	4.845	0.999	0.078	0.972	0.142	0.037	0.931	

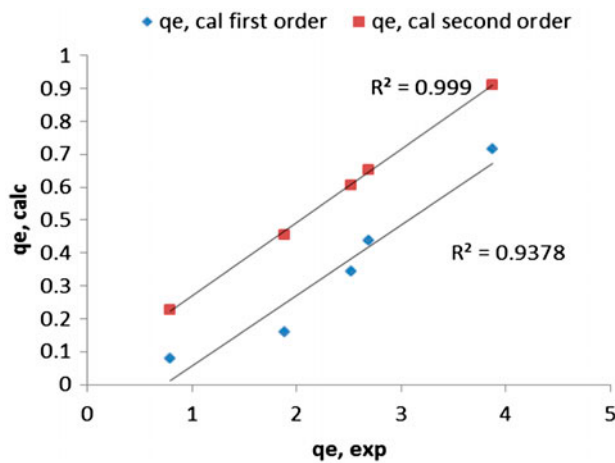


Fig. 15. Comparison of experimental and predicted values of q_e .

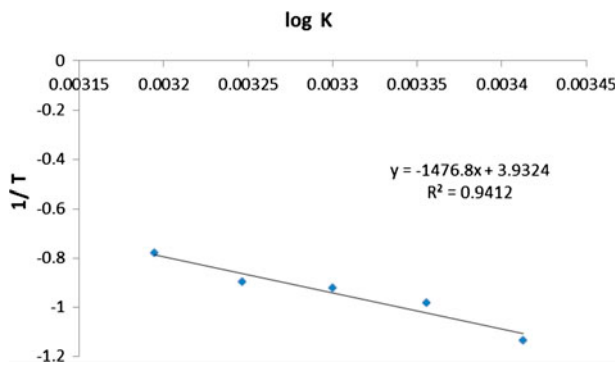


Fig. 16. Van't Hoff plot of $\log K$ vs. $1/T$.

rate-controlling step [37]. The comparison of experimental and predicted values of q_e is shown in Fig. 15. The R^2 values from Table 4 shows better fitting of first-order kinetics for adsorption of dyes on fly ash.

3.6. Thermodynamic studies

Thermodynamic parameters such as change in standard Gibbs free energy (ΔG°), standard enthalpy (ΔH°), and standard entropy (ΔS°) were calculated from experimental data at different temperatures. The change in Gibbs free energy (ΔG°) is related to the equilibrium constant K by the Van't Hoff equation as follows [38]:

$$\Delta G^\circ = -RT \ln K \quad (14)$$

where

$$K = \frac{q_e}{C_e} \quad (15)$$

The change in Gibbs free energy (ΔG°) is related to the change in entropy (ΔS°) and the change in enthalpy (ΔH°) by the following equation:

$$\Delta G^\circ = \Delta H^\circ - T\Delta S^\circ \quad (16)$$

Equation (iii) and (v) can be combined and written as:

$$\ln K = \frac{-\Delta G^\circ}{RT} = \frac{\Delta S^\circ}{R} - \frac{\Delta H^\circ}{RT} \quad (17)$$

$$\log K = \frac{\Delta S^\circ}{2.303R} - \frac{\Delta H^\circ}{2.303RT} \quad (18)$$

The value of ΔH° and ΔS° is obtained from the slope and intercept of the linear plot of $\log K$ vs. $1/T$, respectively. A straight line plot was obtained with a regression coefficient of 0.941 as shown in Fig. 16 and the thermodynamic parameters for adsorption of a mixture of dyes on fly ash are given in Table 5. The positive value of ΔH° indicates that the process is endothermic in nature and the positive value of ΔS° indicates the increased randomness at the solid/solution interface during the adsorption of the dye onto

Table 5
Thermodynamic parameters for the adsorption of mixture of dyes onto fly ash

Temperature (K)	K (L/g)	ΔG° (kJ/mol)	ΔH° (kJ/mol)	ΔS° (J/mol K)
293	0.0728	-6.3825	28.2765	75.2942
298	0.1038	-5.5128		
303	0.1195	-5.3520		
308	0.1267	-5.2895		
313	0.1661	-4.6710		

Table 6
Characterization of effluent

S. No.	Particulars	Before treatment	After treatment
1	pH	7.41	6.9
2	Chemical oxygen demand (ppm)	1,023	243
3	Biochemical oxygen demand (ppm)	231	66
4	Color (PCU)	342	25

fly ash. While, the negative values of ΔG° indicate the feasibility of the process and the spontaneous nature of the adsorption [39,40].

3.7. Characterization of effluent of handmade paper industry

The effluent of handmade paper using mixture of direct orange, direct navy blue, and direct violet dye was characterized before and after fly ash treatment under optimum conditions and the results are given in Table 6.

4. Conclusion

The present study shows that coal fly ash is an effective low-cost adsorbent for the removal of a mixture of dyes compared to the expensive activated carbon. A high value of R^2 (0.993) shows good fitting of the Langmuir isotherm (Q_{\max} value of 120.482 mg/g) with the experimental data representing monolayer adsorption. The amount of dye adsorbed q_e at a pH of 6.0 (2.60 mg/g) was marginally below the amount of dye adsorbed at pH 2 (3.64 mg/g) indicating the field applicability for the treatment of industrial waste at pH 6. However, the maximum adsorption capacity was found at fly ash dosage of 40 g/L having particle size of 45–75 μm with dye solution at pH 2 and 40°C temperature. The kinetic sorption data are well represented by the pseudo-second-order kinetics for the entire sorption period. The E value of 0.7 kJ/mol from Dubinin–Radushkevich model indicates adsorption of a mixture of dyes on fly ash as physisorption process. The values of the different thermodynamic parameters, i.e. the change in enthalpy, entropy, and free energy were evaluated, which indicated that the sorption process is endothermic, spontaneous, and feasible in nature.

Acknowledgment

The authors are highly thankful to Department of Science & Technology for providing financial support

for the study and Material Research Centre, Malaviya National Institute of Technology Jaipur to conduct SEM-EDX, XRD, and FTIR studies.

List of notations

Q_{\max}	— maximum monolayer adsorption capacity (mg/g)
K_L	— Langmuir adsorption constant (l/mg) related to the energy of adsorption
Q_e	— amount of adsorbate adsorbed per unit weight of the adsorbent at equilibrium time (mg/g) from the solution with the equilibrium concentration
C_e	— equilibrium concentration (mg/L)
K_F	— Freundlich adsorption constant (l/mg) which indicates adsorption capacity
$1/n$	— measure of the adsorption density
C_o	— initial concentration of the adsorbate in the solution
q_t	— amount of dye adsorbed (mg/g) at any time t
K_{ad}	— pseudo-first-order rate constant (1/min)
t	— contact time (min)
k_2	— rate constant of pseudo-second-order adsorption (g/mg min)
R	— gas constant (8,314 J/kmol)
T	— absolute temperature (K)
V	— volume of solution (ml)
M	— weight of adsorbent per liter of solution (g/L)
k_0	— Bangham constants
q_s	— theoretical isotherm saturation capacity (mg/g)
K_{ad}	— Dubinin–Radushkevich isotherm constant (mol^2/kJ^2)
ϵ	— Dubinin–Radushkevich isotherm constant
B_{DR}	— isotherm constant

References

- [1] M. Visa, C. Bogatu, A. Duta, Simultaneous adsorption of dyes and heavy metals from multicomponent solutions using fly ash, *Appl. Surf. Sci.* 256 (2010) 5486–5491.
- [2] E. Demirbas, M.Z. Nas, Batch kinetic and equilibrium studies of adsorption of Reactive Blue 21 by fly ash and sepiolite, *Desalination* 243 (2009) 8–21.
- [3] M.T. Yagub, T.K. Sen, S. Afroze, H.M. Ang, Dye and its removal from aqueous solution by adsorption: A review, *Adv. Colloid Interface Sci.* 209 (2014) 172–184.

- [4] M. Visa, Tailoring fly ash activated with bentonite as adsorbent for complex wastewater treatment, *Appl. Surf. Sci.* 263 (2012) 753–762.
- [5] A.R. Dincer, Y. Gunes, N. Karakaya, E. Gunes, Comparison of activated carbon and bottom ash for removal of reactive dye from aqueous solution, *Biore-sour. Technol.* 98 (2007) 834–839.
- [6] P. Janos, H. Buchtova, M. Ryznarova, Sorption of dyes from aqueous solutions onto fly ash, *Water Res.* 37 (2003) 4938–4944.
- [7] E. Voudrias, K. Fytianos, E. Bozaniet, Sorption desorption isotherms of dyes from aqueous solutions and wastewaters with different sorbent materials, *Global Nest Int. J.* 4 (2002) 75–83.
- [8] D. Mohan, K.P. Singh, G. Singh, K. Kumar, Removal of dyes from wastewater using flyash, a low-cost adsorbent, *Ind. Eng. Chem. Res.* 41 (2002) 3688–3695.
- [9] T.A. Khan, I. Ali, V.V. Singh, S. Sharma, Utilization of fly ash as low cost adsorbent for the removal of methylene blue, malachite green and rhodamine B dyes from textile wastewater, *J. Environ. Prot. Sci.* 3 (2009) 11–22.
- [10] A.A. Ramezani-pour, *Cement Replacement Materials*, Springer Geochemistry/Mineralogy, Springer-Verlag, Berlin Heidelberg, 2014, pp. 48–50.
- [11] M.M. Maroto-Valer, D.N. Taulbee, J.C. Hower, Characterization of differing forms of unburned carbon present in fly ash separated by density gradient centrifugation, *Fuel* 80 (2001) 795–800.
- [12] E. Papachristou-Koloveva, *The Use of Fly Ash for Lead Removal from Industrial Wastes*, PhD Dissertation, Aristotle University of Thessaloniki, Thessaloniki, Greece, 1982, 76–79.
- [13] A. Kulkarni, S. Raje, J. Peerzada, M. Rajgor, A miniscule endeavour for accomplishing hypo sludge fly ash brick in Indian context, *Int. J. Eng. Trends Technol.* 10 (2014) 361–365.
- [14] S. Yadav, S. Agnihotri, S. Gupta, R.K. Tripathi, Incorporation of STP sludge and Fly ash in brick manufacturing: An attempt to save the environment, *Int. J. Adv. Res. Technol.* 3 (2014) 138–144.
- [15] A. Dutta, M. Visa, Simultaneous removal of two industrial dyes by adsorption and photo-catalysis on a fly-ash-TiO₂ composite, *J. Photochem. Photobiol. A: Chem.* 306 (2015) 21–30.
- [16] M. Visa, L. Isac, A. Duta, New fly ash TiO₂ composite for the sustainable treatment of wastewater with complex pollutants load, *Appl. Surf. Sci.* 339 (2015) 62–68.
- [17] I.D. Mall, V.C. Srivastava, N.K. Agarwal, I.M. Mishra, Adsorptive removal of malachite green dye from aqueous solution by bagasse fly ash and activated carbon-kinetic study and equilibrium isotherm analyses, *Colloids Surf., A* 264 (2005) 17–28.
- [18] S. Kara, C. Aydinler, E. Demirbas, M. Kobya, N. Dizge, Modeling the effects of adsorbent dose and particle size on the adsorption of reactive textile dyes by fly ash, *Desalination* 212 (2007) 282–293.
- [19] S. Banerjee, M.C. Chattopadhyaya, Adsorption characteristics for the removal of toxic dye, tartrazine from aqueous solutions by a low cost agricultural by-product, *Arabian J. Chem.* (2013) (Article in press), doi: 10.1016/j.arabjc.2013.06.005.
- [20] S.K. Sonar, P.S. Niphadkar, S.M. Mayadevi, P.N. Joshi, Preparation and characterization of porous fly ash/NiFe₂O₄ composite: Promising adsorbent for the removal of Congo red dye from aqueous solution, *Mater. Chem. Phys.* 148 (2014) 371–379.
- [21] B. Acemioğlu, Adsorption of Congo red from aqueous solution onto calcium-rich fly ash, *J. Colloid Interface Sci.* 274 (2004) 371–379.
- [22] L.S. Yadav, B.K. Mishra, A. Kumar, K.K. Paul, Arsenic removal using bagasse fly ash-iron coated and sponge iron char, *J. Environ. Chem. Eng.* 2 (2014) 1467–1473.
- [23] V.C. Srivastava, I.D. Mall, I.M. Mishra, Treatment of pulp and paper mill wastewaters with poly aluminium chloride and bagasse fly ash, *Colloids Surf., A* 260 (2005) 17–28.
- [24] L. Wei, K. Wang, Q. Zhao, C. Xie, W. Qiu, T. Jia, Kinetics and equilibrium of adsorption of dissolved organic matter fractions from secondary effluent by fly ash, *J. Environ. Sci.* 23 (2011) 1057–1065.
- [25] M.I. Temkin, V. Pyzhev, Kinetics of ammonia synthesis on promoted iron catalyst, *Acta Phys. Chim.* 12 (1940) 327–356.
- [26] C. Aharoni, M. Ungarish, Kinetics of activated chemisorption. Part 2. Theoretical models, *J. Chem. Soc. Faraday Trans.* 73 (1977) 456–464.
- [27] A. Günay, E. Arslankaya, İ. Tosun, Lead removal from aqueous solution by natural and pretreated clinoptilolite: Adsorption equilibrium and kinetics, *J. Hazard. Mater.* 146 (2007) 362–371.
- [28] A. Dąbrowski, Adsorption—From theory to practice, *Adv. Colloid Interface Sci.* 93 (2001) 135–224.
- [29] J.C. Igwe, A.A. Abia, Adsorption isotherm studies of Cd(II), Pb(II) and Zn(II) ions bioremediation from aqueous solution using unmodified and EDTA-modified maize cob, *Eclética Quím.* 32 (2007) 33–42.
- [30] M.M. Dubinin, The potential theory of adsorption of gases and vapors for adsorbents with energetically nonuniform surfaces, *Chem. Rev.* 60 (1960) 235–241.
- [31] J.P. Hobson, Physical adsorption isotherms extending from ultrahigh vacuum to vapor pressure, *J. Phys. Chem.* 73 (1969) 2720–2727.
- [32] K.Y. Foo, B.H. Hameed, Insights into the modeling of adsorption isotherm systems, *Chem. Eng. J.* 156 (2010) 2–10.
- [33] A.O. Olalekan, A.P. Olatunya, A.M. Dada, O. Dada, Langmuir, Freundlich, Temkin and Dubinin-Radushkevich isotherms studies of equilibrium sorption of Zn²⁺ onto phosphoric acid modified rice husk, *IOSR J. Appl. Chem.* 3 (2012) 38–45.
- [34] K. Badii, F.D. Ardejani, M.A. Saberi, N.Y. Limaee, S.Z. Shafaei, Adsorption of acid blue 5 dye on diatomite in aqueous solutions, *Ind. J. Chem. Technol.* 17 (2010) 7–16.
- [35] Y.S. Ho, G. McKay, Sorption of dye from aqueous solution by peat, *Chem. Eng. J.* 70 (1998) 115–124.
- [36] C. Aharoni, S. Sideman, E. Hoffer, Adsorption of phosphate ions by colloid ion coated alumina, *J. Chem. Technol. Biotechnol.* 29 (1979) 404–412.
- [37] I.D. Mall, V.C. Srivastava, N.K. Agarwal, Removal of Orange G and Methyl Violet dyes by adsorption onto bagasse fly ash-kinetic study and equilibrium isotherm analyses, *Dyes Pigment.* 69 (2006) 210–223.

- [38] V.S. Mane, I.D. Mall, V.C. Srivastava, Use of bagasse fly ash as an adsorbent for the removal of brilliant green dye from aqueous solution, *Dyes Pigm.* 73 (2007) 269–278.
- [39] P. Pengthamkeerati, T. Satapanajaru, N. Chatsatapatayakul, P. Chairattanamanokorn, N. Sananwai, Alkaline treatment of biomass fly ash for reactive dye removal from aqueous solution, *Desalination* 261 (2010) 34–40.
- [40] S. Agarwal, K. Singh, A.B. Gupta, A.K. Sharma, Fly ash as low cost adsorbent for treatment of effluent of handmade paper industry-Kinetic and modelling studies for direct black dye, *J. Cleaner Prod.* 112 (2016) 1227–1240.